

CHEMISTRY

A European Journal

A Journal of



Accepted Article

Title: How inter- and intramolecular reactions dominate formation of products in lignin pyrolysis

Authors: Victoria B.F. Custodis, Patrick Hemberger, and Jeroen A. van Bokhoven

This manuscript has been accepted after peer review and appears as an Accepted Article online prior to editing, proofing, and formal publication of the final Version of Record (VoR). This work is currently citable by using the Digital Object Identifier (DOI) given below. The VoR will be published online in Early View as soon as possible and may be different to this Accepted Article as a result of editing. Readers should obtain the VoR from the journal website shown below when it is published to ensure accuracy of information. The authors are responsible for the content of this Accepted Article.

To be cited as: *Chem. Eur. J.* 10.1002/chem.201700639

Link to VoR: <http://dx.doi.org/10.1002/chem.201700639>

Supported by
ACES

WILEY-VCH

How inter- and intramolecular reactions dominate formation of products in lignin pyrolysis

Victoria B. F. Custodis^[a,c], Patrick Hemberger^[b] and Jeroen A. van Bokhoven^[a,c,*]

Abstract: One of the key challenges in renewable chemical production is the conversion of lignin, especially by fast pyrolysis. The complexity of the lignin pyrolysis process has prevented the identification of the mechanism, inhibiting further industrial implementation. By combining pyrolysis of model compounds (4-phenoxyphenol and 2-methoxy-phenoxybenzene) with lignin bonds characteristic under vacuum and realistic pressure conditions, the roles of inter- and intramolecular reactions were established. On the one hand the stable 4-O-5 ether bond enables, without breaking, C-C bond formation and even directly forms naphthalene depending on the position and type of the substituent. P-benzoquinone intermediates, on the other hand are highly unstable at ambient pressure and directly decompose into coke and carbon monoxide. The system pressure (radical concentration) plays a crucial role in the dominant reaction mechanism by initiating intramolecular reactions, interfering with intramolecular reactions. H-transfer and recombination reactions suppress the decarbonylation of phenoxy radicals, thus yielding a very different product distribution.

Introduction

Lignin is one of three main components lignocellulosic biomass and is regarded to be the largest renewable biofuel in Europe (2007).^[1] Pulp and paper mills produce a surplus of energy by simple incineration. The specific structure of lignin makes it a possible source of chemicals. It has high potential as a feedstock for bulk and fine chemicals, especially aromatic and phenolic compounds.^{[2],[3]} Lignin is polymerized from three phenolic monomers, resulting in a complex and irregular polymer that is very hard to characterize.^[4] Scheme 1 is a sample sketch of the lignin polymer together with the three building blocks: coniferyl, sinapyl and coumaryl units. Prominent bonds are β -O-4 (aryl ether), α -O-4 (aryl ether), 4-O-5 (aromatic ether), 5-5 (C-C aromatic) or spiro-bonds (C-C). The lignin structure varies depending on the bioresource and separation method as well as storage time. Model compounds are commonly studied to understand chemical upgrading and

depolymerization and enable the study of a single bond or building block. Due to the complexity and diversity of the lignin many chemical reactions and processes occur simultaneously during lignin treatment, so that specific behavior is generally hard to correlate to one chemical/physical property of the lignin.^[5,6] Model compounds, such as guaiacol and diphenylether resemble a common intermediate (and building block) and the 4-O-5 bond.

Fast pyrolysis, in particular fast pyrolysis, is a promising method to depolymerize lignin with all its different bonds to obtain valuable chemicals.^[7] Here, the lignin polymer is thermally broken down and yields a mix of oxygen-containing molecules, mostly phenols. Thermal-induced decomposition of macromolecules results from the formation of radicals, which can recombine easily and, in times form undesired char. The liquid product of fast pyrolysis is bio-oil, which is unstable and corrosive. A great deal of research has been devoted to the improvement of the quality of the products, as well as to a decrease in char by catalytic fast pyrolysis (CFP).^[7-12]

Both pyrolysis and catalytic pyrolysis depend on the thermal depolymerization of the lignin polymer. The mechanism of depolymerization and monomer formation is crucial to predict and ultimately to influence product selectivity. The quantitative and qualitative characterization of the radical depolymerization of the lignin polymer is very difficult.^[13] Thus, typical monomers are investigated instead.

Many model compounds have been studied: phenylphenylether,^{[14],[15]} diphenylether, phenol,^[16,17] anisole,^[18-20] and guaiacol.^[21,22] These model compounds represent a typical feature of lignin, such as frequently occurring bonds, building blocks or a component of the pyrolysis oil.^[15,23] Brebu et al.^[24] give a summary of many model compound studies. Phenylphenylether (PPE) is the model compound mimicking the β -O-4 bond and its decomposition mechanism depends strongly on the temperature. Extensive studies have shown that there are two dominating mechanisms, the 6-centred retro-ene and the Maccoll elimination,^[25,26] both of which lead to phenol and styrene as end-products.^[27,28] The β -O-4 bond is only present in small quantities in most industrial lignins, since it can be easily hydrolysed during the separation process.^[29] Phenol, a very simple model compound, forms cyclopentadienyl radicals by decarbonylation.^{12,17} Guaiacol also decarbonylates after phenoxy formation under collision reduced-conditions. Collision-reduced conditions exist when the sample concentration is very low and the vacuum high, so that direct radicals are detectable, because they are not quenched by bimolecular reactions.^[31,32]

[a] Victoria B. F. Custodis and Prof. Dr. Jeroen A. van Bokhoven, Institute for Chemical and Bioengineering, Department of Chemistry and Applied Biosciences, ETH Zurich, HCI E 127, Vladimir-Prelog-Weg 1, 8093 Zurich, Switzerland.
jeroen.vanbokhoven@chem.ethz.ch

[b] Dr. Patrick Hemberger, Laboratory for Femtochemistry and Synchrotron Radiation, Paul Scherrer Institute, CH-5232 Villigen-PSI, Switzerland

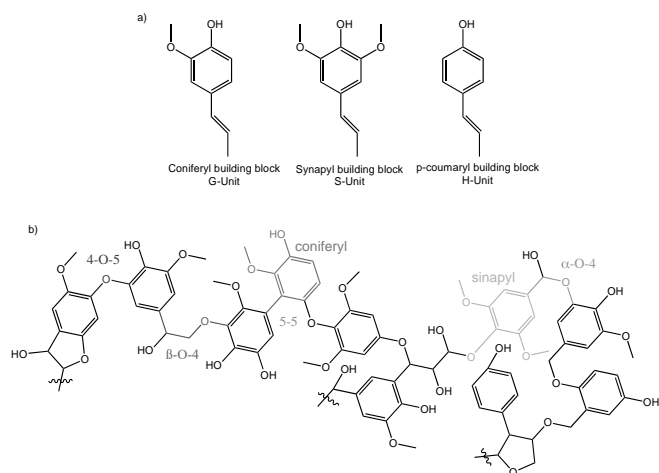
[c] Prof. Dr. J. A. van Bokhoven, Laboratory for Catalysis and Sustainable Chemistry, Paul Scherrer Institute, WLG 135, 5232 Villigen, Switzerland.

Supporting information for this article is given via a link at the end of the document.

FULL PAPER

WILEY-VCH

This study will focus on the most stable ether bond, the 4-O-5 bond, which is even more stable than some C-C bonds.^[33] Which primary radicals form and in which further reactions do they participate? Aim is to control those intermediates and to steer the reactions towards producing more valuable products.



Scheme 1. a) building blocks and b) lignin sample structure.

There are two possible approaches to studying the pyrolysis mechanism of lignin. Top down: looking at all the radicals of the lignin during pyrolysis,^[13,34,35] or bottom up: focusing on one model compound at a time.^[31,32,36] Both approaches have advantages and disadvantages. On the one hand, information is incomplete, when only the integrated signal of all the different components are determined, while on the other hand, many side-reactions and other components are ignored in hope of representing the major component. This conflict is particularly evident in research on lignin due to its heterogeneity. We focus on both approaches and their differences in order to identify possible dependencies and connections.

We employed two types of pyrolysis setups, which detect isolated radicals as well as the stable end-products: py-GC/MS at ambient pressure and iPEPICO at the VUV (x04db) beamline of the Swiss Light Source under reactive collision-reduced conditions. Py-GC/MS detects products of recombination, rearrangement and stabilization. In contrast, in the iPEPICO setup, the detection of molecules is so immediate and the residence time in the reactor is so short (hundreds of microseconds) that even radicals are detectable. The iPEPICO system determines each radical and intermediate by threshold photoelectron spectra (TPES) isomer-specifically.^[37] iPEPICO yields the reaction mechanisms of the initial reactions and py-GC/MS the stabilized products. This combination bridges the pressure gap and enables identification of the role of reaction conditions on mechanisms and possible products.

We determine the importance of hydroxyl and methoxy substituents on the model dimers 4-phenoxyphenol and 1-methoxy-2-phenoxybenzene and how they affect the decomposition pathway and the breakup of the stable aromatic ether bond. The radical environment, in our case the strong dilution of the model compound vs. ambient pressure, is crucial to take into account during the thermal degradation of lignin. Previous studies have shown that selectivity not only depends

on the kinetics of the decomposition mechanism, but also relies strongly on the environment, especially in radical reactions.^[32,35] Ambient pressure enhances bimolecular reactions and in particular H-transfer and -loss become important radical transfer and formation steps, while the monomolecular decomposition at high vacuum depends mainly on homolytic fission of the weakest bond.

Results and Discussion

Results

4-phenoxyphenol (PhOPhOH)

Figure 1 shows the most common products detected upon fast pyrolysis of 4-phenoxyphenol in the py-GC/MS setup. First decomposition was observed at temperatures higher than 600 °C during pyrolysis. The first products were phenol, benzene and dibenzofuran. The phenol selectivity decreases quickly with temperature, while benzene selectivity increases steadily. Other minor products above 800 °C are toluene, styrene, diphenylether, indene, hydroxyl-biphenyl and anthracene. Above 800 °C, a noticeable amount of biphenyl forms, and at 850 °C naphthalene and more benzene forms. The pyrolysis temperatures are considerably high, which is necessary, because this compound evaporates very quickly.

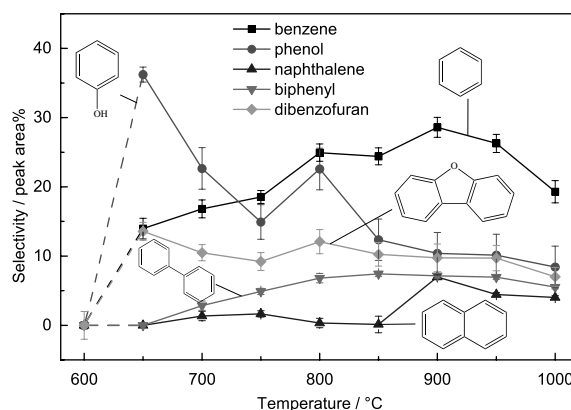


Figure 1. Product selectivity of the main products of 4-phenoxyphenol pyrolysis at different temperatures and at ambient pressure in py-GC/MS.

Figure 2 shows the relative signals (normalized to total peak area) at each pyrolysis temperature under high vacuum at a constant sample temperature and 10.5 eV ingoing photon energy. The relative signal strength mirrors the mechanism in terms of primary, secondary and tertiary products. At the lowest temperature, at which the parent molecule decomposes, various products emerge: $m/z=108/109$, $m/z=93$, $m/z=80$, $m/z=77$, $m/z=65$ and $m/z=52$. According to their ionization energy and TPE spectra at 760 °C the products are the hydroxyl-phenoxy radical (109), p-benzoquinone (108), the phenoxy radical (93), cyclopentadienone (80), the phenyl radical (77), cyclopentadienyl radical (65) and butane-3-yne (52). Some of these species are known from the decomposition of guaiacol and could be identified based on previous studies and recorded spectra.^[31,32]

FULL PAPER

WILEY-VCH

Above 750 °C, $m/z=39$, propargyl radicals, are also detected as well as $m/z=26$, which is acetylene and is not visible in Figure 2, since it ionizes only above 11.4 eV. At 820 °C, the signal at $m/z=186$ (PhOPhOH) almost depleted, indicating complete decomposition of the parent molecule. Additional measurements at 13.9 eV and 14.1eV photon energy, at 760 °C, revealed also the formation of carbon monoxide, $m/z=28$.

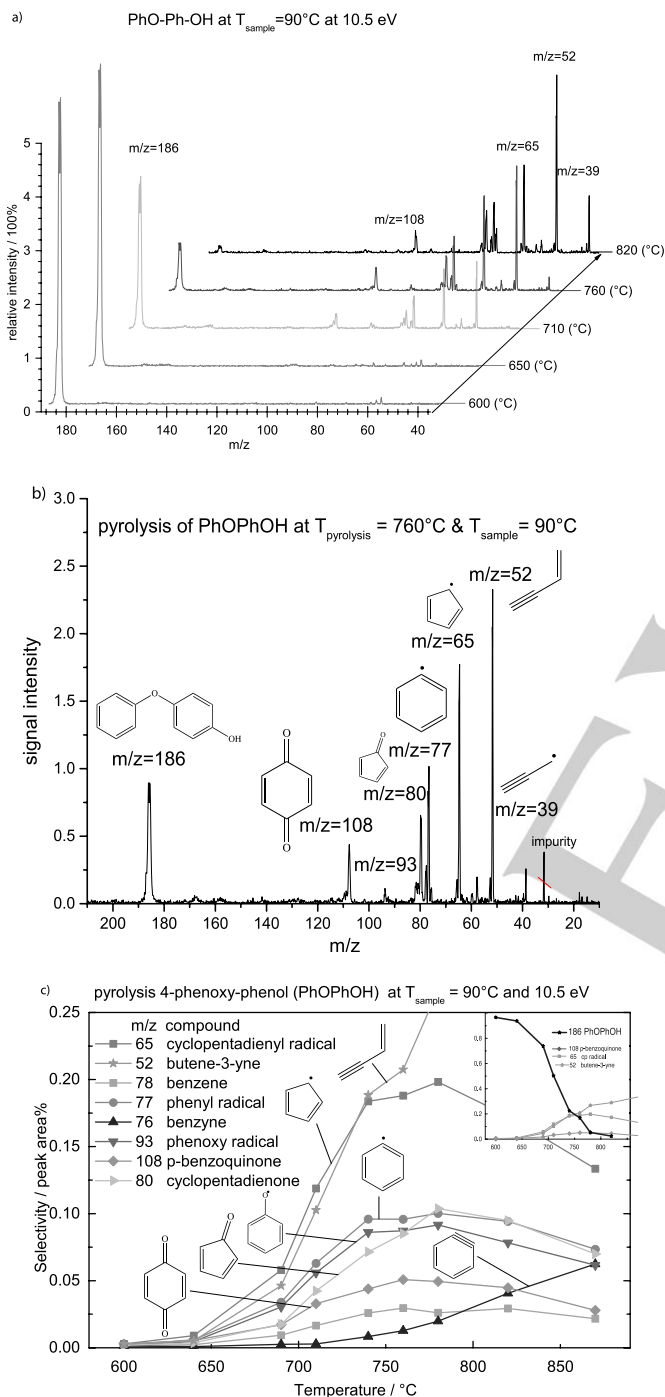


Figure 2. a) Temperature-dependent mass spectra in the iPEPICO-TOF setup at a sample temperature of 90°C and an ionization beam energy of 10.5eV and b) a detailed mass spectrum at 760°C. c) Thermal breakdown diagram with primary and secondary products using the iPEPICO setup. Data is on the integration of the mass spectra from $T_{\text{sample}} = 90^\circ\text{C}$ and 10.5 eV

Figure 2c shows the fractional abundances (relative selectivities by peak-areas) of the ionized products and intermediates. Due to the different ionization cross-sections of each molecule the signal intensity alone provides only limited quantitative information. However, if the ionization energy and the inlet stream are kept constant, the relative increase and decrease in signal intensity identifies reaction sequences. As the parent signal decreases, all products form at the same pyrolysis temperature (640 °C). The relative increase of the cyclopentadienyl radical and the butene-3-yne is the steepest, followed by phenoxy and phenyl radicals. Above 750 °C phenyl radicals and the benzene signals decrease, and benzyne ($m/z=76$) is detected. In general, the phenyl and phenoxy radicals as well as benzoquinone and benzene show similar trends, while cyclopentadienone ($m/z=80$) and benzyne ($m/z=76$) peak at higher temperatures.

Comparing the products in the iPEPICO experiment (Fig 2b) there is a lack of benzoquinone (BQ) and benzenediol products in py-GC/MS. Further investigations with pyrolysis of a mixture of PhOPhOH and p-benzoquinone at ambient pressure showed high conversion of the quinone (over 60% at 700°C compared to 8% BQ alone), while most of it converted to coke and trace amounts (< 0.05 peak area %) of products. Copyrolysis led to an increase in carbon monoxide up to 2 mol % compared to 0.04 mol % (PhOPhOH) and 0.16 mol % (BQ).

1-methoxy-2-phenoxybenzene (PhOPhOMe)

PhOPhOMe at ambient pressure (py-GC/MS) decomposes in a different way to 2-phenoxy-phenol and dibenzofuran-2-ol. Figure 3 shows that the primary product is the corresponding hydroxide 2-phenoxyphenol. At very low conversion, this is the only product besides recombination products and 2-hydroxyphenyl-phenylmethanone. At higher temperatures selectivity of dibenzofuranol and dibenzofuran increases, while that of 2-phenoxyphenol decreases. Benzene, dibenzodioxin and phenols are also detected, the latter being mainly phenol and trace amounts of methyl-phenols. Even though 2-phenoxy-phenol is a major intermediate in py-GC/MS, the other products do not decompose in the same way as 4-phenoxyphenol.

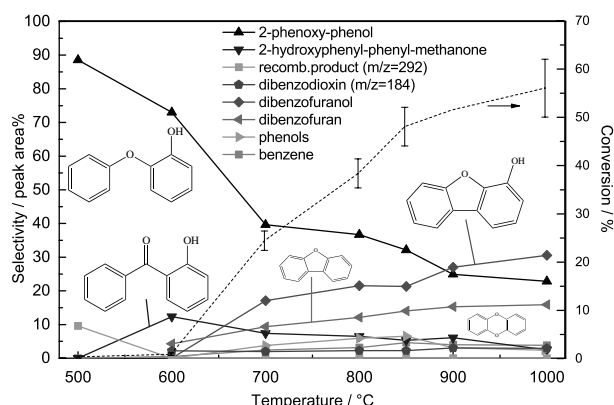


Figure 3. Product selectivity of 1-hydroxy-2-phenoxybenzene (PhOPhOMe) pyrolysis in py-GC/MS at ambient pressure) as dependent on the temperature.

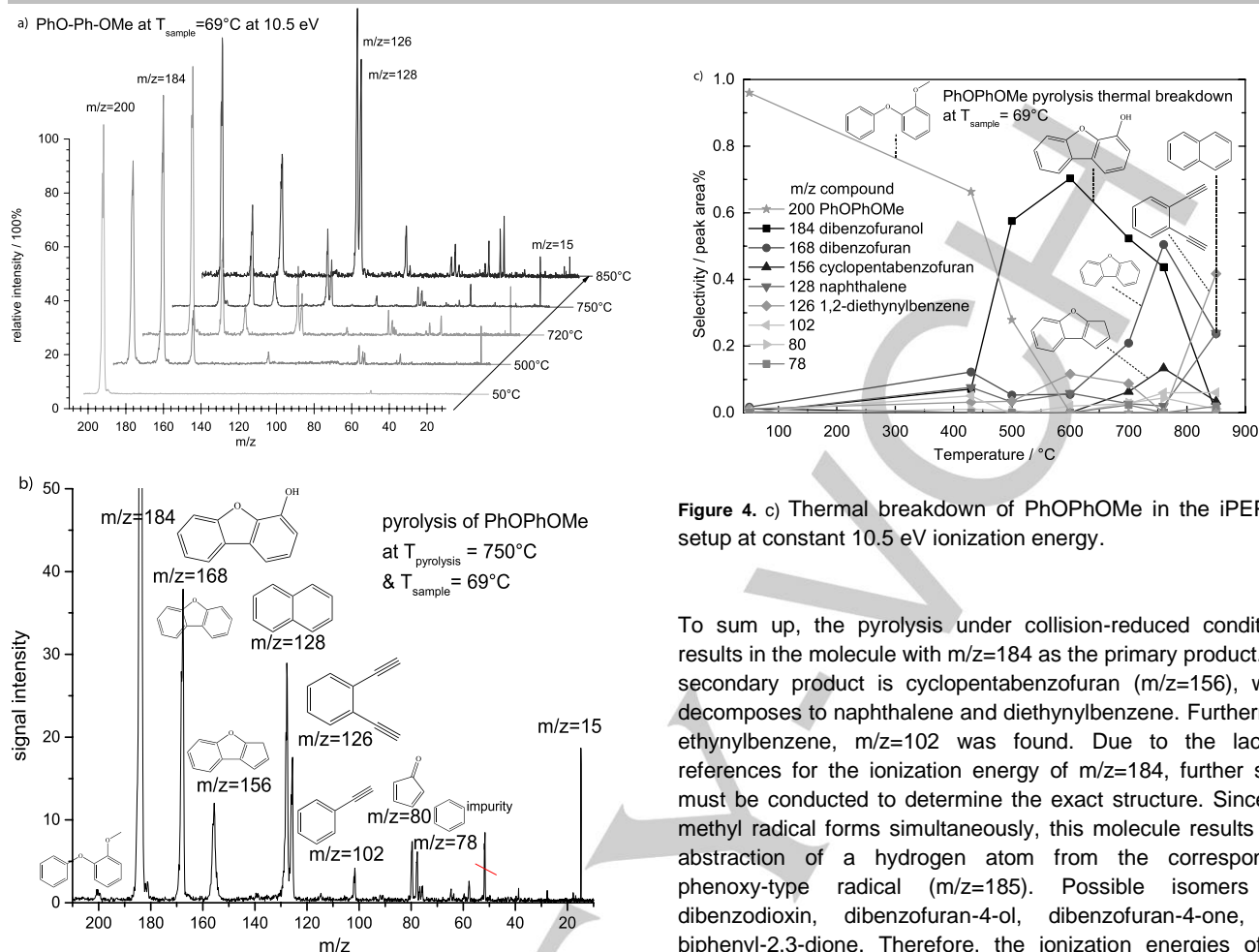


Figure 4. a) Temperature-dependent mass spectra (normalized to the highest peak) of the pyrolysis of PhOPhOMe in the iPEPICO-TOF setup at a sample temperature of 90 °C and an ionization beam energy of 10.5 eV and b) a detailed mass spectrum at 750 °C.

Figure 4a shows the primary products of 1-methoxy-2-phenoxybenzene (PhOPhOMe), measured in iPEPICO under high vacuum. Figure 4b shows the detailed mass spectrum of the products at 750 °C. At this temperature, the parent molecule decomposes almost completely, and the signal at $m/z=200$ is quite low. The detected product molecules and radicals are $m/z=184/185$, $m/z=168$ (dibenzofuran), $m/z=156$, $m/z=128$ (naphthalene), $m/z=126$ (diethynylbenzene), $m/z=102$ (ethynylbenzene), and $m/z=15$ (methyl radical). Small amounts of $m/z=78/77$ and $m/z=80$ are also observed *vide infra*. As soon as PhOPhOMe starts to decompose the molecule $m/z=184$ forms. $m/z=185$ is detected and its mass spectrum shown in Figure S1 (Supplemental Information). Furthermore, the methyl radical, $m/z=15$, is visible from the start ($T = 500$ °C). As temperature increases the molecule with $m/z=156$ forms and decomposes again above 750 °C. At this temperature naphthalene and diethenyl benzene are the main products.

Figure 4. c) Thermal breakdown of PhOPhOMe in the iPEPICO setup at constant 10.5 eV ionization energy.

To sum up, the pyrolysis under collision-reduced conditions, results in the molecule with $m/z=184$ as the primary product. The secondary product is cyclopentabenzofuran ($m/z=156$), which decomposes to naphthalene and diethynylbenzene. Furthermore ethynylbenzene, $m/z=102$ was found. Due to the lack of references for the ionization energy of $m/z=184$, further study must be conducted to determine the exact structure. Since the methyl radical forms simultaneously, this molecule results from abstraction of a hydrogen atom from the corresponding phenoxy-type radical ($m/z=185$). Possible isomers are dibenzodioxin, dibenzofuran-4-ol, dibenzofuran-4-one, and biphenyl-2,3-dione. Therefore, the ionization energies of the listed isomers were calculated using Gaussian09 on the CBS-QB3 level of theory. Table S1 gives the calculated ionization energies (IE) and the experimental value of $m/z=184$ (8.03eV). Dibenzodioxin shows an IE of 7.48 eV (7.5 eV in literature).^[38] Dibenzofuranol has a calculated IE of 8.06 eV, dibenzofuran-4-one 7.74 eV, and biphenyl-2,3-one 8.45 eV. For the intermediate with $m/z=156$ the structure of cyclopenta-benzofuran was reconstructed, which shows an experimental ionization energy of 7.5 eV, while the calculated energy was 7.49 eV(B3LYP) and 7.42 eV(CBS-QB3).

Based on the calculations, the isomer with the best fit, dibenzofuran-4-ol, was synthesized and its TPES measured and compared to the experimental TPES of the intermediate product during pyrolysis of PhOPhOMe at 750 °C. The spectra in Figure S2 show good agreement. Dibenzofuran-4-ol pyrolysis, also yields the following familiar fragments: first $m/z=156$, then $m/z=128$ (naphthalene) and $m/z=126$ (diethynylbenzene) followed by $m/z=102$ (ethynylbenzene). Figure S3 shows the corresponding mass spectra. Those detected products are the same as in PhOPhOMe pyrolysis, which again proves that dibenzofuran-4-ol is the main intermediate with $m/z=184$. We have performed quantum chemical calculations to evaluate reaction pathways yielding dibenzodioxin and dibenzofuran-4-ol, which clearly favors the latter one as presented in Figure 5. While the formation of a new ether bond (R4) is less energetically demanding than the H transfer, the hydrogen abstraction in the second step requires much more energy than the hydrogen abstraction of R3 to form dibenzofuranol.

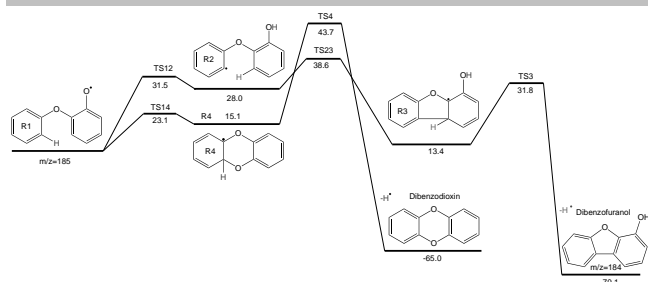


Figure 5. Reaction pathways to dibenzodioxin and dibenzofuranol initiated by methyl abstraction from 1,2-methoxy-phenoxybenzene. The latter pathway is favored by around 5 kcal/mol. All energies are given in kcal/mol.

Discussion

4-phenoxyphenol

Due to the introduction of a hydroxyl group to the diphenylether^[32] and similar bond energies of the ether bonds two reaction pathways can open up, which are depicted in Figure 6. We can now determine how this dimer decomposes at elevated temperatures and introduce a (temperature dependent) decomposition mechanism and show how the primary radicals convert into stable products at ambient pressure. Phenyl radical loss (Figure 6, route a on the right) affords p-hydroxyphenoxy radicals, which yields benzoquinone after further hydrogen abstraction as commonly observed in lignin pyrolysis.^[39] The quinone usually remains in the polymer and contributes to the char.^[35] In the following, the reactions of the benzoquinone and phenoxy radicals are discussed explaining the induced selectivity of the intermediately generated radicals.

Figure 6 shows the decomposition mechanism of PhOPhOH under vacuum with all the detected intermediates. As mentioned before, all fragments are detected at the same temperature. Therefore, both reaction pathways (a and b) are energetically equal. In pathway b the carbon-based hydroxyphenyl radical rearranges immediately to the most stable C₆H₅O isomer, the phenoxy radical (Figure 6, on the left).^[40]

Also at ambient pressure both fission pathways are observed, as benzene and phenol appear simultaneously. However, stabilized equivalents of the phenoxy-hydroxy radical or benzoquinone were not observed. The benzoquinone is known to decompose quickly to carbon monoxide and butane-3-yne^[36] and carbon monoxide was detected in both experimental setups (in py-GC/MS max 0.07 mol%), but can be found in both reaction pathways.

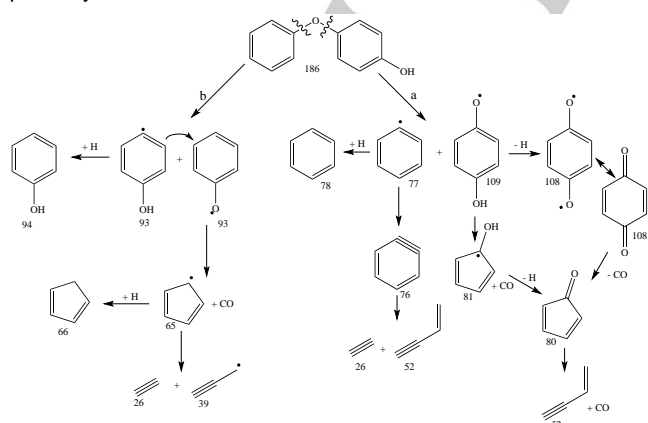


Figure 6. Decomposition mechanism and fission pathways of 4-hydroxyphenol (PhOPhOH), deduced from the iPEPICO experiments.

The fragments butene-3-yne and the cyclopentadienyl (cp) radical are unique in pathway a) and b) respectively. Pathway b) leads to the immediate formation of the cp radical, which is known to dimerize to form naphthalene and coke.^[20] At ambient pressure (Figure 1) phenol forms and accordingly phenoxy radicals are stabilized by H-addition first - and only above a certain temperature the phenoxy-radicals react further to dimerization. As usual the five-ring species evade detection in the py-GC/MS-setup.^[31,32] In contrast, in the PEPICO experiment, the phenoxy radical thermalizes and immediately decomposes to cp and even smaller radical fragments (m/z=39 and m/z=26) at higher temperatures.^[40,41] Similarly to the decomposition of guaiacol^[32] we see immediately that intermolecular radical reactions play an important role in pyrolysis under actual conditions and prevent fragmentation into molecules smaller than aromatics.

When stabilization by H-addition (radical transfer reactions) is apparently common in a radical-rich environment, the question arises, why the hydroxy-phenoxy radical is not stabilized by the same quenching pathway forming 1,4-benzenediol. The latter radical was also stabilized by H-abstraction to form benzoquinone, which evades detection in py-GC/MS similar to the five-ring species. The mere presence of benzene and biphenyl products in py-GC/MS proves the existence of the second decomposition pathway a). In pyrolysis tests at ambient pressure the benzoquinone cannot be detected anymore in the presence of 4-phenoxyphenol. In a reactive environment quinones may quickly be depleted to yield carbon monoxide or recombine to naphthalene-dione, styrene or naphthalene. The increased reactivity of benzoquinone (BQ) in copyrolysis may explain why it was not detected by GC/MS. Upon guaiacol pyrolysis, the similar ortho hydroxyl-phenoxy radicals cannot be detected, but the corresponding o-benzenediol, especially at elevated temperatures (ambient pressure).^[32] Robichaud et al. detected p-benzoquinone in p-dimethoxybenzene pyrolysis; it decomposes further to cyclopentadienone and butane-3-yne.^[36] In their study kinetic calculations showed that the formation of p-benzoquinone is 10⁶ times faster than its decomposition by decarbonylation.^[36,42] The absence of benzoquinone in the GC/MS emphasizes the large difference between theoretically favored reaction pathways and actual reactivity in the radical, gas phase environment. While stabilization to benzoquinone is, in theory, much more likely, the product is hardly detected.

1,2-methoxy-phenoxybenzene

The methoxy substitution of diphenylether in ortho position is a common moiety in lignin.^[24,43] Both the methoxy-group and the ether bond are possible breaking points in this model compound. However O-CH₃ bond cleavage is favored, due to the formation of resonantly stabilized phenoxy-like radicals. The latter intermediate may also yield the corresponding o-benzoquinone.^[35] In the following we will discuss the different reaction pathways and why o-benzoquinone is not favored, but a new carbon-carbon bond is formed accompanied by the usual decarbonylation.^[40,44] Furthermore, we will augment our analytical observations by quantum chemical calculations, providing evidence why the pathway to dibenzofuranol is favored.

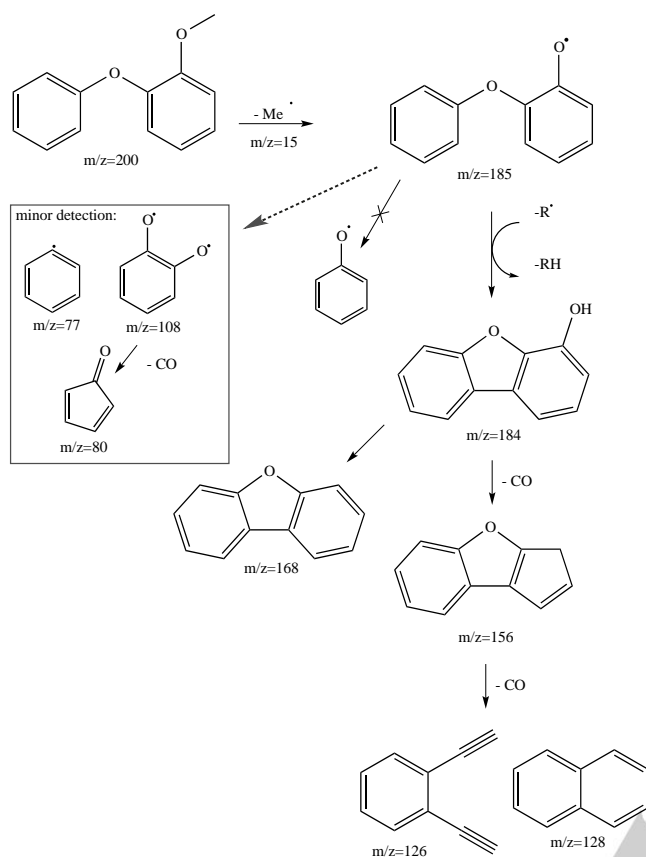


Figure 7. Decomposition mechanism of 1-methoxy-2-phenoxybenzene in collision reduced conditions deduced from the results in iPEPICO experiments.

Figure 7 summarizes the decomposition of 1-methoxy-2-phenoxybenzene and radical intermediates as detected by iPEPICO experiment. In contrast to 4-phenoxyphenol, the primary intermediate radical $m/z=185$ is indeed very unstable, but does not break up at the ether bond to form phenoxy-like radicals as 4-phenoxyphenol does. There is a side reaction, similar to pathway b) (Figure 6) in PhOPhOH, which revealed by the presence of cyclopentadienone and phenyl radicals/benzene in trace amounts. The o-quinone with $m/z=108$ was not detected, but it probably reacted further as quickly as it is formed, as similar observations have been made together with kinetic calculations with methoxy-phenoxy radicals.^[36] However, the major decomposition pathway at low pressure, does not involve break-up of the ether bond but internal stabilization by abstraction of hydrogen. The thermal energy required to dissociate the methoxy group is clearly sufficient for the molecule to form a new intramolecular C-C bond, which leads directly to the formation of naphthalene. Quantum chemical calculations show that the formation of dibenzofuranol requires less activation energy via several transition states and the H-transfer to the new hydroxyl-group. The first step on the way to dibenzodioxin requires indeed less energy (R4, Figure 5), but is outcompeted by the lower activation barrier to yield dibenzofuranol (TS3, Figure 5). At higher temperatures and a denser environment with more bimolecular reactions, H-abstraction may be favored and more dibenzodioxin can indeed be observed compared to the low pressure of the pyrolysis reactor in the iPEPICO experiment.

Altarawneh et al. also calculated the various possibilities of catechol coupling and concluded that a phenoxy-phenyl radical tends to undergo loss of hydrogen rather than formation of dibenzodioxin as a result of condensation and confirmed by our experimental observations.^[45] The observation of a newly formed C-C bond upon pyrolysis is striking, because it shows that this molecule is able to form naphthalene, a precursor of char, even unimolecularly. The phenyl-ether radical may form such products easily because of low activation energy.^[46] Compared to other lignin dimers, such as phenyl-phenethyl-ether, the ether bond is so stable especially with a more fragile MeO-substituent, that its thermal breakup involves the formation of a new carbon-carbon bond. This is different compared to non-substituted diphenylether, which showed major recombination at high pressure and lower temperature.^[32]

The further decomposition of PhOPhOMe is, as in previous studies, dominated by decarbonylation under high vacuum. Furthermore, similar to guaiacol decomposition at ambient pressure, 2-hydroxyphenyl-phenylmethanone is detected at lower temperatures (Figure 3).^[32] This is initiated by radical formation and subsequent 1,2-phenyl shift, similar to the 1,2-methyl shift in guaiacol to yield the corresponding benzaldehyde.^[21,36,47] Figure S4 shows the proposed mechanism. Probably due to the steric hindrance of the phenyl group it is only formed in small quantities and outcompeted by other reactions at higher temperatures. Instead of a methyl shift the whole phenyl ring has to shift in this reaction. As temperature increases dibenzofuranol and dibenzofuran are generated. Dibenzofuranol and the isomer dibenzodioxin are also detected at ambient pressure in contrast to the iPEPICO experiment.

Plain diphenylether decomposes at ambient pressure pyrolysis first and forms larger recombination products (Fig 8) and at higher temperatures dibenzofuran; benzene and phenol are only tertiary products.^[32] When comparing these results with the decomposition of hydroxy and methoxy substituted diphenylether in the same setup, the decomposition temperature decreases from 650 to 600 °C to 500 °C. At ambient pressure the most prominent radical reactions are not induced by the fission of the ether bond, but rather by hydrogen transfer in all the compounds. This always leads to selectivity towards dibenzofuran and dibenzofuranol as secondary products. Comparing those three model compounds, each with a different substituent, PhOPhOH first produces benzene and phenol followed by dibenzofuran (recombination), while diphenylether produces directly recombination products. Methoxy-phenoxybenzene on the other hand, yields the hydroxyl equivalent (2-phenoxyphenol, Fig 3), which means that major fractions of the ether bond remains intact. In lignin pyrolysis hydroxyl groups in the p-position are preferred, because they have the least tendency to recombine or build carbon-carbon bonds. As mentioned above, diphenylether is known to recombine at first and only at higher temperatures and the secondary oligomers are either not formed anymore or decompose faster than they are formed.^[32] However, this plain model compound is unlikely to exist in real lignin. Most phenols in lignin have both methoxy and hydroxyl groups. Lignin with p-coumaryl subunits (H-units) usually occur in grasses and for example miscanthus,^[48] which however have a low lignin content. In general, the 4-O-5 bond is present in most lignins by 5 to 10% per 100 C9 units.^[48] This may not be the major fraction of bond

type, but the presence of this bond in real lignin will either lead to recombination and dibenzofuran-like compounds or not to a break-up of the lignin under ambient conditions. The desired monomers thus do not form. Even if a dimer forms with this residual ether bond and even if exists in the polymeric matrix, it will further react to form C-C bonds and will eventually lead to char. The weaker aryl ether bonds (β -O-4 and α -O-4) break down easily by hydrolysis during lignin separation or pretreatment.^[29]

Reactions, which tend to lead to C-C bond formation rather than the breakup of the aromatic ether bond are a major issue during lignin pyrolysis. This aromatic ether bond directly produces carbon-carbon bonds, even in high vacuum. The substituent in this model compound can thus steer the decomposition reactions. The p-hydroxyl group relative to the ether bond leads at first to more monomers, but in a radical environment the p-benzoquinone decomposes directly leading to carbon monoxide and coke as well.

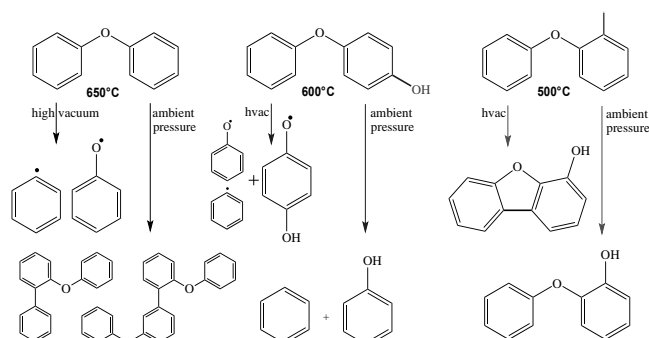


Figure 8. Reaction pathways of the model compounds under various conditions.^[32]

Conclusions

The iPEPICO analytical setup is a powerful tool enabling the determination of complex decomposition mechanism with intermediates unknown to literature. P-phenoxy-phenol breaks up to form phenoxy, phenyl and hydroxyphenoxy radicals, and the o-methoxy-benzene-phenol forms an intramolecular C-C bond, and eventually naphthalene instead of breaking the ether bond of the dimer. The comparison of these results with the products of py-GC/MS reveals the importance of the pressure and thus the radical environment during pyrolysis. Even though the PhOPhOMe forms ortho-PhOPhOH as an intermediate product, the product distribution is very different due to H-transfer reactions at higher pressures preventing further degradation of the dimer. In the lignin polymer, where many more substituents are present and potential H-transfer reactions may occur, the break-up of this ether bond seems even more unlikely. In contrast, the p-hydroxyl substituent leads to fission of the ether bond without these recombination reactions, even at ambient pressure. However, the resulting benzoquinone is highly unstable in a radical environment and decomposes immediately to carbon monoxide and char. Therefore, the aromatic ether bond present in lignin largely influence the lignin depolymerization due to the identified subsequent reactions in this work, which do not only depend on pressure, radical concentration, but also on the type and position of the substituent in lignin. A suitable pretreatment could control

depolymerization and repolymerization rates and thus product selectivity to a larger extend than the mere percentage of this ether bond in lignin.

Experimental Section

Materials

The model compounds are 4-phenoxyphenol (PhOPhOH) (>99 %, ABCR Chemicals), dibenzo-p-dioxin (>99 %, TCI Europe). All quartz devices were calcined before reaction in air at 550°C for 5h at a heating rate of 5°C/min. The following compounds were synthesized:

1-phenoxy-2-methoxybenzene

1-phenoxy-2-methoxybenzene (PhOPhOMe) was synthesized according to Evans et al.^[49] by esterification from guaiacol and phenylboronic acid. Guaiacol and benzenboronic acid (AlfaAesar, >98 %), together with triethylamine and Cu(OAc)₂, were stirred in dichloromethane for 18h in a nitrogen atmosphere and with 4Å molecular sieve. After chromatographic purification and recrystallization white crystals formed with a purity of > 99.5 % by GC/MS. The characterization of 1-phenoxy-2-methoxybenzene was also done by ¹H- and ¹³C-NMR.

dibenzofuran-4-ol

Dibenzofuran-4-ol (4-hydroxybenzofuran) was synthesized according to Shultz et al.^[50] by oxidation of the corresponding boronic acid with hydrogen peroxide in tetrahydrofuran.

4-(dibenzofuran-2-yl)boronic acid (Sigma Aldrich, > 95 %) was diluted in THF, a 2 % NaOH solution and five times molar excess of H₂O₂ in a nitrogen atmosphere and stirred at room temperature for 24 h. After removing THF by vacuum, the organic product was extracted with diethylether and washed with water and recrystallized over night. Purity and identity were determined by GC/MS, ¹H and ¹³C NMR.

iPEPICO experiment and VUV-Beamline

To investigate the primary thermal decomposition mechanism, pyrolysis of 4-phenoxyphenol and 1-phenoxy-2-methoxybenzene was performed in the iPEPICO-endstation^[37,51] of the VUV-Beamline at the Swiss Light Source.^[52] The X04DB bending magnet provides the synchrotron radiation collimated by a toroidal mirror onto a 150 l/mm grating. Another mirror focuses the radiation on the exit slits, which together with a mixture of neon, argon and krypton are in the gas-filter. The latter one suppresses the high order radiation, which is also diffracted by the grating. The pyrolysis setup consists of an resistively heated SiC-tube (1 mm iD / 2 mm oD, 10 mm heated zone).^[32] An argon stream carries the diluted (>0.1 %) starting material through the reactor resulting in average residence times of 100-300 μ s. A typical backing pressure of 500 mbar was applied to the 100 μ m nozzle generating a supersonic molecular beam going through the reactor and into the iPEPICO source chamber at 10⁻⁴ mbar. The molecular beam enters the spectrometer chamber (1.5 x 10⁻⁶ mbar) after skimming and is subsequently ionized by VUV light. The photon-energy resolution is typically around 8 meV, which is calibrated according to the Rydberg state of argon. The electrons are velocity map imaged and detected by a Roentdek DLD40 position sensitive detector and the corresponding ions, detected in a Jordan TOF (C-726) mass spectrometer, accelerate in the opposite direction. A multiple start – multiple stop scheme correlates the events in real time.^[53] To identify isomers and intermediates mass-selected TPES were recorded with a resolution of 0.01 eV. The background of hot electrons is subtracted according to the method from Sztaray and Baer.^[54]

FULL PAPER

WILEY-VCH

Signals are considered to be impurities, when the signal intensity does not depend on the pressure - and therefore the concentration - of the molecular inlet beam, which means that those compounds are in the detector chamber and do not influence the reaction. Additionally, experiments with varying sample concentrations (backing pressure of the molecular beam) were performed in order to rule out possible changes in selectivity due to bimolecular collisions. In the tested range limited by the vapor pressure of the model compound no changes were observed.

Py-GC/MS

Ambient pressure pyrolysis of the model compounds was performed in a platinum coil pyrolyzer (5150, CDS Analytical) consisting of an open-ended quartz reactor packed with loose quartz-wool in a helium carrier gas stream. The model compound (1-2 μL) was pyrolyzed at a heating rate of 20 $^{\circ}\text{C}/\text{ms}$, and was then kept at the final temperature for 1 min. The pyrolysis products were injected into an Agilent 7890A GC with an Agilent 5975C MS system through the pyrolysis interface and transfer line at 300 $^{\circ}\text{C}$. The GC also has a thermal conductivity detector (TCD), which is calibrated for the most predominant gases (CO , CO_2 , CH_4 etc.). The condensable fraction injected into the GC/MS system was characterized according to the NIST08 mass spectrum library. The stated selectivity was based on the percentage of the peak area and the conversion was calculated by the integrated peak area. Variation of the sample size at 900 $^{\circ}\text{C}$ determined the standard deviation of each product. All reactions were at least performed in duplicate and reproduced within 95 %.

Gaussian calculations

Gaussian 09 was utilized, applying the B3LYP functional and the 6-311++G(d,p) basis set to calculate the equilibrium geometry and force constant matrixes^{[55]a}, which were used to compute Franck-Condon factors with the ezSpectrum.OSX program.^{[55]a,b} To calculate the ionization energies and the relative energy differences of unknown intermediates the CBS-QB3 composite method was selected.^[56,57]

Acknowledgements

The authors thank the Swiss National Science Foundation for financial support (NRP66, no. 406640-136892). The experiments were performed at the VUV beamline of the Swiss Light Source at the Paul Scherrer Institute (PSI). The work was supported financially by the Swiss Federal Office for Energy (BFE Contract Number SI/501269-01). Calculations were performed at the HPC cluster Brutus at ETH.

Keywords: lignin • fast pyrolysis • model compounds • radical mechanism • TPES iPEPICO

- [1] J. Jönsson, K. Pettersson, T. Berntsson, S. Harvey, *Int. J. Energy Res.* **2013**, *37*, 1017–1035.
- [2] A. V. Bridgwater, *Biomass and Bioenergy* **2012**, *38*, 68–94.
- [3] T. Dickerson, J. Soria, *Energies* **2013**, *6*, 514–538.
- [4] K. Freudenberg, H. Richtzenhain, *Angew. Chemie* **1939**, 1–5.
- [5] O. Faix, *Holzforchung* **1991**, *45*, Suppl. 21–27.
- [6] V. B. F. Custodis, C. Bährle, F. Vogel, J. A. van Bokhoven, *J. Anal. Appl. Pyrolysis* **2015**, *115*, 214–223.
- [7] T. P. Vispute, H. Zhang, A. Sanna, R. Xiao, G. W. Huber, *Science* **2010**, *330*, 1222–7.
- [8] T. R. Carlson, G. A. Tompsett, W. C. Conner, G. W. Huber, *Top. Catal.* **2009**, *52*, 241–252.
- [9] Z. Ma, E. Troussard, J. A. van Bokhoven, *Appl. Catal. A Gen.* **2012**, *423–424*, 130–136.
- [10] D. J. Mihalcik, C. A. Mullen, A. A. Boateng, *J. Anal. Appl. Pyrolysis* **2011**, *92*, 224–232.
- [11] M. Zhang, F. L. P. Resende, A. Moutsoglou, D. E. Raynie, *J. Anal. Appl. Pyrolysis* **2012**, *98*, 65–71.
- [12] D. M. Alonso, J. Q. Bond, J. A. Dumesic, *Green Chem.* **2010**, *12*, 1493–1513.
- [13] C. Bährle, T. U. Nick, M. Bennati, G. Jeschke, F. Vogel, *J. Phys. Chem. A* **2015**, *119*, 6475–6482.
- [14] A. Demirbas, *Energy Sources, Part A Recover. Util. Environ. Eff.* **2009**, *31*, 1186–1193.
- [15] C. Zhao, J. A. Lercher, *Angew. Chemie* **2012**, *124*, 6037–6042.
- [16] A. B. Lovell, K. Brezinsky, I. Glassman, *Int. J. Chem. Kinet.* **1989**, *21*, 547–560.
- [17] A. M. Scheer, C. Mukarakate, D. J. Robichaud, M. R. Nimlos, H.-H. Carstensen, G. B. Ellison, *J. Chem. Phys.* **2012**, *136*, 44309.
- [18] E. Barker Hemings, G. Bozzano, M. Dente, E. Ranzi, *Chem. Eng. Trans.* **2011**, *24*, 61–66.
- [19] M. M. Suryan, *J. Am. Chem. Soc.* **1989**, *111*, 1423–1429.
- [20] A. V. Friderichsen, E. J. Shin, R. J. Evans, M. R. Nimlos, D. C. Dayton, G. B. Ellison, *Fuel* **2001**, *80*, 1747–1755.
- [21] P. F. Britt, A. C. Buchanan, M. J. Cooney, D. R. Martineau, *J. Org. Chem.* **2000**, *65*, 1376–89.
- [22] P. F. Britt, A. C. Buchanan, K. B. Thomas, S.-K. Lee, *J. Anal. Appl. Pyrolysis* **1995**, *33*, 1–19.
- [23] M. Koyama, *Bioresour. Technol.* **1993**, *44*, 209–215.
- [24] M. Brebu, C. Vasile, *Cellul. Chem. Technol.* **2010**, *44*, 353–363.
- [25] A. Maccoll, S. W. Ramsay, R. F. Laboratories, W. C. I. London, *Chem. Rev.* **1969**, *69*, 33.
- [26] H. Kwart, S. F. Sarner, J. Slutsky, R. December, *J. Am. Chem. Soc.* **1973**, *95*, 5234–5242.
- [27] M. T. Klein, P. S. Virk, *Ind. Eng. Chem. Fundam.* **1983**, *22*, 35–45.
- [28] M. W. Jarvis, J. W. Daily, H.-H. Carstensen, A. M. Dean, S. Sharma, D. C. Dayton, D. J. Robichaud, M. R. Nimlos, *J. Phys. Chem. A* **2011**, *115*, 428–438.
- [29] B. Saake, R. Lehen, *Ullmann's Encycl.* **2012**, 21–36.
- [30] A. Beste, A. C. Buchanan, *J. Phys. Chem. A* **2012**, *116*, 12242–8.
- [31] A. M. Scheer, C. Mukarakate, D. J. Robichaud, M. R. Nimlos, G. B. Ellison, *J. Phys. Chem. A* **2011**, *115*, 13381–9.
- [32] V. B. F. Custodis, P. Hemberger, Z. Ma, J. A. van Bokhoven, *J. Phys. Chem. B* **2014**, *118*, 8524–8531.
- [33] R. Parthasarathi, R. A. Romero, A. Redondo, S. Gnanakaran, *J. Phys. Chem. Lett.* **2011**, *2*, 2660–2666.
- [34] C. Bährle, V. Custodis, G. Jeschke, J. A. van Bokhoven, F. Vogel, *ChemSusChem* **2016**, *9*, 2397–2403.
- [35] C. Bährle, V. Custodis, G. Jeschke, J. A. van Bokhoven, F. Vogel, *ChemSusChem* **2014**, *7*, 2022–9.
- [36] D. J. Robichaud, A. M. Scheer, C. Mukarakate, T. K. Ormond, G. T. Buckingham, G. B. Ellison, M. R. Nimlos, *J. Chem. Phys.* **2014**, *140*, 234302.
- [37] A. Bodi, P. Hemberger, T. Gerber, B. Sztáray, *Rev. Sci. Instrum.* **2012**, *83*, 83105.
- [38] F. P. Colonna, G. Distefano, V. Galasso, K. J. Irgolic, C. E. King, G. C. Pappalardo, *J. Organomet. Chem.* **1978**, *146*, 235–244.
- [39] E. Dorrestijn, L. J. J. Laarhoven, I. W. C. E. Arends, P. Mulder, *J. Anal. Appl. Pyrolysis* **2000**, *54*, 153–192.
- [40] P. Hemberger, G. da Silva, A. J. Trevitt, T. Gerber, A. Bodi, *Phys.*

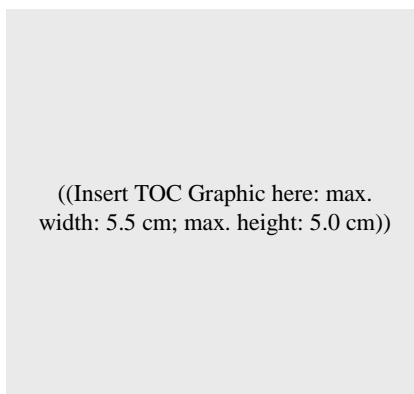
- Chem. Chem. Phys.* **2015**, *17*, 30076–30083.
- [41] T. K. Ormond, P. Hemberger, T. P. Troy, M. Ahmed, J. F. Stanton, G. B. Ellison, *Mol. Phys.* **2015**, *113*, 2350–2358.
- [42] P. Frank, J. Herzler, T. Just, C. Wahl, *Symp. Combust.* **1994**, *25*, 833–840.
- [43] R. Rinaldi, R. Jastrzebski, M. T. Clough, J. Ralph, M. Kennema, P. C. A. Bruijninx, B. M. Weckhuysen, *Angew. Chemie Int. Ed.* **2016**, *55*, 8164.
- [44] H.-H. Carstensen, A. M. Dean, *Int. J. Chem. Kinet.* **2011**, *41*, 498–506.
- [45] M. Altarawneh, B. Z. Dlugogorski, *Phys. Chem. Chem. Phys.* **2015**, *17*, 1822–30.
- [46] S. Li, Q. Zhang, *Comput. Theor. Chem.* **2015**, *1061*, 80–88.
- [47] E. Dorrestijn, P. Mulder, *J. Chem. Soc. Perkin Trans. 2* **1999**, 777–780.
- [48] A. J. Ragauskas, G. T. Beckham, M. J. Biddy, R. Chandra, F. Chen, M. F. Davis, B. H. Davison, R. A. Dixon, P. Gilna, M. Keller, et al., *Science* **2014**, *344*, 1246843.
- [49] D. A. Evans, J. L. Katz, T. R. West, *Tetrahedron Lett.* **1998**, *39*, 2937–2940.
- [50] D. A. Shultz, J. C. Sloop, G. Washington, *J. Org. Chem.* **2006**, *71*, 9104–13.
- [51] A. Bodi, M. Johnson, T. Gerber, Z. Gengeliczki, B. Sztáray, T. Baer, *Rev. Sci. Instrum.* **2009**, *80*, 34101.
- [52] M. Johnson, A. Bodi, L. Schulz, T. Gerber, *Nucl. Instruments Methods Phys. Res. Sect. A Accel. Spectrometers, Detect. Assoc. Equip.* **2009**, *610*, 597–603.
- [53] A. Bodi, B. Sztáray, T. Baer, M. Johnson, T. Gerber, *Rev. Sci. Instrum.* **2007**, *78*, 84102.
- [54] B. Sztáray, T. Baer, *Rev. Sci. Instrum.* **2003**, *74*, 3763–3768.
- [55] V. Mozhayskiy, A. I. Krylov, **2009**.
- [56] L. A. Curtiss, P. C. Redfern, K. Raghavachari, *J. Chem. Phys.* **2007**, *127*, 124105.
- [57] J. A. Montgomery, M. J. Frisch, J. W. Ochterski, G. A. Petersson, *J. Chem. Phys.* **1999**, *110*, 2822.

Entry for the Table of Contents (Please choose one layout)

Layout 1:

FULL PAPER

Text for Table of Contents



Author(s), Corresponding Author(s)*

Page No. – Page No.

Title

Layout 2:

FULL PAPER

Author(s), Corresponding Author(s)*

Page No. – Page No.

Title

